

Synthesis of hydroxyapatite by hydrothermal and microwave irradiation methods from biogenic calcium source varying pH and synthesis time

Mário Andreato Macedo Castro^{a,*}, Thayane Oliveira Portela^a, Gricirene S. Correa^a,
 Marcelo Moizinho Oliveira^a, José Hilton Gomes Rangel^b, Samuel Filgueiras Rodrigues^a,
 José Manuel Rivas Mercury^a

^a Postgraduate Program in Materials Engineering – PPGEM/IFMA-Monte Castelo, Av. Getúlio Vargas 04, São Luís, Brazil

^b Postgraduate Program in Chemistry – PPGQ/IFMA-Monte Castelo, Av. Getúlio Vargas 04, São Luís, Brazil

ARTICLE INFO

Article history:

Received 29 April 2020

Accepted 30 June 2020

Available online 23 July 2020

Keywords:

Hydroxyapatite

Eggshell

Hydrothermal

Microwave

ABSTRACT

Hydroxyapatite is the main bones and teeth inorganic mineral component. This material has been an object of research aiming its use in biomaterials as bone replacement option for biomedical applications. In this investigation, the synthesis of hydroxyapatite was studied by the Hydrothermal (HT) and Microwave Irradiation (MW) methods. Here, parameters such as pH (9 and 11) and synthesis time were varied, and residue of chicken eggshell was used as calcium precursor. The obtained powders were characterized by X-ray Diffraction (XRD), Fourier Transform Infrared Spectroscopy (FTIR), Dispersive Energy X-ray Spectroscopy (EDS), and Transmission Electron Microscopy (TEM). The results showed that the material synthesized when the pH reached the value of 9 which generated less carbonated powders than those with pH of 11. The Hydrothermal method presented more satisfactory morphological results according to the TEM analysis. This procedure was considered more suitable as a route to obtain hydroxyapatite as biomaterial.

© 2020 SECV. Published by Elsevier España, S.L.U. This is an open access article under the CC BY-NC-ND license (<http://creativecommons.org/licenses/by-nc-nd/4.0/>).

Síntesis de hidroxiapatita por métodos hidrotermal e irradiación de microondas a partir de una fuente de calcio biogénico variando el pH y el tiempo de síntesis

RESUMEN

La hidroxiapatita es el principal componente mineral inorgánico de huesos y dientes. Este material ha sido objeto de investigación dirigida a su uso en biomateriales como sustituto óseo en aplicaciones biomédicas. En este trabajo, se estudió la síntesis de hidroxiapatita utilizando los métodos hidrotermal (HT) y de irradiación de microondas (MW), variando parámetros como el pH (9 y 11) y el tiempo de síntesis, utilizando como precursor de calcio,

Palabras clave:

Hidroxiapatita

Cáscara de huevo

Hidrotermal

Microondas

* Corresponding author.

E-mail address: marioandreato10@hotmail.com (M.A.M. Castro).

<https://doi.org/10.1016/j.bsecv.2020.06.003>

0366-3175/© 2020 SECV. Published by Elsevier España, S.L.U. This is an open access article under the CC BY-NC-ND license (<http://creativecommons.org/licenses/by-nc-nd/4.0/>).

el residuo de la cáscara de huevo de gallina. Los sólidos (polvo) obtenidos se caracterizaron por difracción de rayos X (DRX), espectroscopía infrarroja por transformada de Fourier (FTIR), espectroscopía de energía dispersiva (EDS) y microscopía electrónica de transmisión (MET). Los resultados mostraron que el material sintetizado a pH 9 generó polvos menos carbonatados que aquellos obtenidos a pH 11. El método hidrotérmico presentó resultados morfológicos más satisfactorios según el análisis de MET. Este procedimiento se consideró más adecuado como una ruta para obtener hidroxiapatita como biomaterial.

© 2020 SECV. Publicado por Elsevier España, S.L.U. Este es un artículo Open Access bajo la licencia CC BY-NC-ND (<http://creativecommons.org/licenses/by-nc-nd/4.0/>).

Introduction

Hydroxyapatite ($\text{Ca}_{10}(\text{PO}_4)_6(\text{OH})_2$ - P63/m - Ca/P = 1.67) is a calcium phosphate that has been studied for decades due to its diversity. Among some applications, it is worth mentioning biomaterials in bone grafts and dental coatings [1,2], removal of contaminants in soil and water [3], catalysis of organic compounds and others [4]. Several synthesis methods such as solid-state reaction, mechanochemical synthesis [5,6], combustion in solution, pyrolysis [7,8], sol-gel, microemulsion, hydrothermal method and microwave irradiation [9–11] have been used as techniques to obtain this phosphate.

In Hydrothermal synthesis, the reaction is conducted in the presence of water at temperature range 80–400 °C, pressure up to 100 KPa and prolonged period of times [12]. The hydroxyapatite nanoparticles powders produced in this method are relatively stoichiometric and present high crystallinity. In addition, the phase purity and Ca/P ratio are significantly improved as the hydrothermal time and temperature are increased [13]. In contrast, the synthesis with microwave irradiation is characterized by the in situ microwave energy conversion into heat. Few minutes are required to reach the entire solution volume treatment temperature without any gradient [14]. The hydroxyapatite prepared by this technique, generally contains smaller particle size, good purity and a closer size distribution [13].

The choice of calcium as precursor raw material is extremely important in order to obtain the hydroxyapatite as it often influences the stoichiometry as well as the purity of the material. Chicken eggshells are mainly composed of calcium carbonate (95–97%) which can therefore be adapted as a biogenic source of calcium for the synthesis of hydroxyapatite. In addition, as it is an abundant industrial waste, its use as a raw material for calcium phosphates is a good alternative [15–17]. Other studies showed that hydroxyapatite based on this biogenic source, presents rapid biomineralization when in contact with human tissue, improved mechanical properties and superior sinterability when compared to this compound from inorganic sources [18]. Moreover, Krishna et al. [19] reported that its biocompatibility when extracted from the eggshell, favors the osteoblast cells adhesion and it is non-cytotoxic due to the CaCO_3 biological nature.

When synthesizing hydroxyapatite, parameters such as pH and synthesis time can influence the material properties. Liu et al. [20], using the Hydrothermal method, fixed the synthesis temperature at 140 °C and used pHs of 6, 9 and 14. The produced material exhibited stick-like dispersed

particles, and the degree of agglomeration grown up as the pH increased. When using microwave irradiation synthesis, Wang et al. [21], chose temperatures of 100, 120 and 140 °C and times of 1 and 30 min. The obtained hydroxyapatite compound presented crystal growth proportional to time and temperature and stick-like morphologies.

In this work, hydroxyapatite powders produced by hydrothermal and microwave irradiation hydrothermal were synthesized using chicken eggshells as a biogenic source. Parameters such as pH and synthesis time were varied during the investigations.

Materials and methods

Obtaining calcium precursor

Chicken eggshells were collected, washed by using distilled water and later had their membranes removed. Then, the shells were boiled in a mixture of distilled water and ethanol to remove impurities and organic residues followed by drying process at 100 °C for 24 h. The dried shells were grounded in agate mortar to produce fine particulate powder.

For the formation of $\text{Ca}(\text{OH})_2$, 11 g of the eggshell powder was dissolved into 209 mL of hydrochloric acid (HCl, PA, Neon, Brazil) at a concentration of 0.8 mol L^{-1} under stirring at 40 °C for 1 h. Then, an 80 mL solution of 1.09 mol L^{-1} sodium hydroxide (NaOH, Macron, Brazil) was added. Finally, the precipitate was filtered and dried at 100 °C in an oven for 24 h.

Synthesis of hydroxyapatite

In order to obtain hydroxyapatite powders, pH parameters, temperature and time for conventional hydrothermal and microwave irradiation synthesis were determined. This work is based on previous investigations carried out by Qi et al. [9] who varied the pH in the Hydrothermal synthesis, Méndez-Lozano et al. [22] who applied different synthesis times by Microwave Irradiation, Nga et al. [23] who used several times in the Hydrothermal synthesis, and Rivera et al. [24] who altered the pHs in the Microwave Irradiation synthesis.

The synthesis of hydroxyapatite was performed starting from equal volume precursor solutions containing 0.0279 mol of calcium hydroxide ($\text{Ca}(\text{OH})_2$) and 0.0167 mol of phosphoric acid (H_3PO_4). The molar ratio was kept Ca/P = 1.67 and pH was adjusted to 9 or 11 with ammonium hydroxide solution (1:1). After addition of the precursors, the resulting solution was aged at 80 °C under magnetic stirring for 2 h. This last process

Table 1 – Identification of the samples prepared according to the synthesis method, pH and employed synthesis time.

Method	pH	Synthesis time	Code
Hydrothermal (HT)	9	6 h	HT9-6h
		12 h	HT9-12h
	11	6 h	HT11-6h
		12 h	HT11-12h
Microwave irradiation (MW)	9	1 min	MW9-1min
		36 min	MW9-36min
	11	1 min	MW11-1min
		36 min	MW11-36min

was adopted on the products obtained from the two synthesis methods, so that the powders were better compared.

For the Hydrothermal Synthesis, after the aging period, the precipitate was placed into a Teflon reactor, placed in a stainless steel autoclave and kept in the oven for 6 or 12 h at 180 °C.

Microwave Irradiation synthesis was performed at the end of aging time, at 80 °C with heating ratio of 5 °C min⁻¹, and synthesis times of 1 and 36 minutes. A Panasonic Smart Junior microwave operated under 800 W power and 2.4 GHz frequency was used.

The products obtained from both methods, were filtered and washed three times with distilled water and once with ethanol to remove impurities. Finally, the solid was oven dried at 100 °C for a period of 24 h.

The produced samples were identified according to the different type of synthesis (Hydrothermal – HT, Microwave Irradiation – MW), pH (9 or 11) and synthesis time (6 or 12 h, 1 or 36 min), see Table 1.

Characterizations techniques

X-ray diffraction

The crystalline phases of the eggshell and hydroxyapatite powders were analyzed by X-ray diffraction technique (XRD, Bruker, D8 Advance), CuK α radiation (1.5404 Å), 10–90° scan and step size of 0.02° s⁻¹.

The crystallite size in hydroxyapatite powders was determined from the Scherrer Eq. (1):

$$L = 0.9\lambda / \beta \cos \theta \quad (1)$$

where L is the crystallite size (nm), λ is the wavelength of the electromagnetic radiation used (0.154 nm), β is the width at half height of the highest intensity diffraction peak and θ is the Bragg angle of the highest intensity diffracted peak.

Fourier transform infrared spectroscopy

The functional groups present in hydroxyapatite were determined by Fourier transform infrared spectroscopy (FTIR, Shimadzu, IR-Prestige 21), between 400 and 4000 cm⁻¹.

Carbonate content in the materials was calculated from the FTIR results using the equation of Feathstone et al. [25]. For the calculation, the E_i extinction coefficients of the carbonate

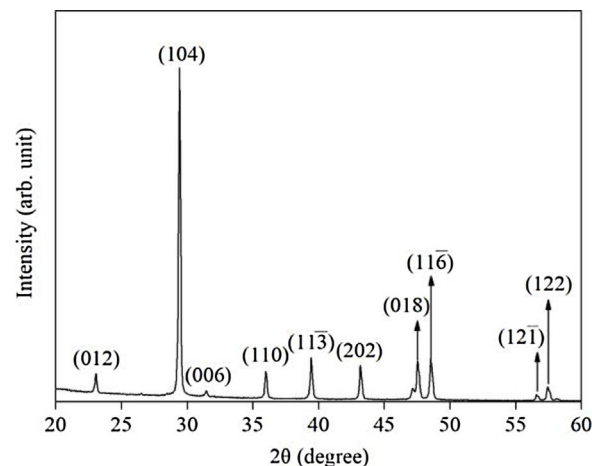


Fig. 1 – X-ray diffraction pattern of eggshell.

band present at or around 1458 cm⁻¹ and the phosphate band at or near 604 cm⁻¹ were obtained using Eqs. (2) and (3):

$$\%CO_3^{2-} = 13.5 \left(\frac{E_{i1458}}{E_{i604}} \right) - 0.2 \quad (2)$$

$$E_i(1458 \text{ or } 604) = \log \left(\frac{T_2}{T_1} \right) \quad (3)$$

Here, T_2 and T_1 are the transmittance at the local baseline (1458 and 604 cm⁻¹) and the corresponding peak (1458 and 604 cm⁻¹), respectively.

Dispersive energy X-ray spectroscopy-EDS

Semiquantitative chemical analysis of the material to obtain the Ca/P ratio was performed using dispersive energy X-ray spectroscopy (EDS, Oxford, Aztec Energy X-Act).

Transmission electron microscopy

The morphology of the powders was observed by transmission electron microscopy (TEM, Jeol, model JEM-2100) and the Image J software was used to calculate the particle size.

Results and discussion

X-ray diffraction (XRD) of the eggshells and hydroxyapatite powders

The XRD results from eggshells are shown in Fig. 1. The image displays the peaks corresponding to calcite (ICDD database 01-072-1937) with rhombohedral crystalline system, proving in this way that the precursor material is mostly calcium, which are similar to previous researchers results [16,19,26].

The XRD patterns of hydroxyapatite powders prepared by the two synthesis methods are shown in Fig. 2. It is noted that no other crystalline phase was detected besides hydroxyapatite, according to ICDD database 01-086-0740. This can be confirmed by the index peaks of Miller (002), (211), (300), (202), (310), (222) and (213) present in all sample standards and confirmed on the material crystallographic sheet [24]. For both employed techniques, the powders presented low

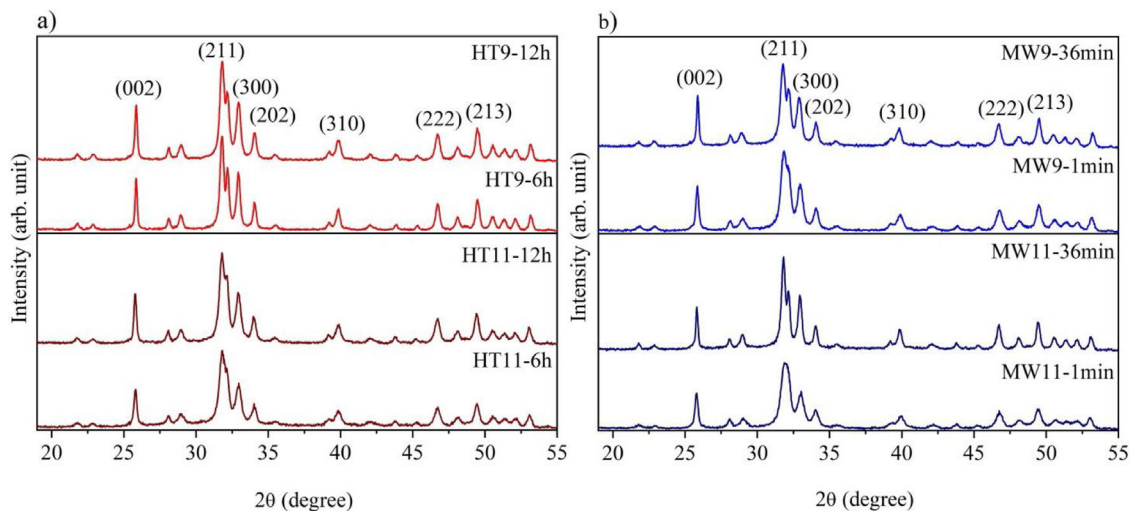


Fig. 2 – X-ray diffraction patterns of hydroxyapatite samples synthesized by (a) hydrothermal and (b) microwave irradiation.

crystallinity at the shortest synthesis times, as evidenced by the wide peaks of the XRD patterns of the samples [27,28]. However, crystallinity improved with synthesis time, which can be observed by increasing the intensity of the main peak (211) and decreasing peak width [29].

Fourier transform infrared spectroscopy

The vibrational spectra obtained by FTIR are depicted in Fig. 3. The bands in the region between 1033 and 1037 cm^{-1} are assigned to the PO_4^{3-} group, and are related to the asymmetrical stretching, ν_3 , of the P–O bonds and 962 cm^{-1} to the symmetrical stretching, ν_1 . An asymmetric flexion, ν_4 , of the O–P–O bond is also observed in the regions of $565\text{--}566\text{ cm}^{-1}$ and $603\text{--}604\text{ cm}^{-1}$ respectively [22,30,31]. The OH^- bands appear in the regions of 3567 cm^{-1} and 671 cm^{-1} refer to the symmetric stretching mode of the hydroxyapatite structural hydroxyl [32,33]. The vibrations of the adsorbed water molecules in the hydroxyapatite structure are present between $1629\text{--}1656\text{ cm}^{-1}$ and $3430\text{--}3456\text{ cm}^{-1}$ [10]. The vibrations of the CO_3^{2-} group appear in the regions between $1458\text{--}1460\text{ cm}^{-1}$ and 874.5 cm^{-1} show that hydroxyapatite is of Type B, i.e. when phosphate ions are replaced by carbonate ions absorbed from the ambient atmosphere during the synthesis of the material [30,34].

Crystal size, estimated carbonate values and Ca/P ratio

Table 2 shows the crystal size, the estimated carbonate values and the Ca/P ratio of all obtained samples. It is noted that the size of the crystal increased with the synthesis time. However, compared to bone hydroxyapatite crystallites, which are in the $20\text{--}40\text{ nm}$ range, three samples with shorter synthesis times (HT9-6 h, MW9-1 min and MW11-1 min) had smaller crystal size [35].

From the estimated carbonate values, it can be seen that the HT11-12 h, MW9-36 min and MW11-36 min samples exceeded the upper limit of the CO_3^{2-} ion present in bone tissue hydroxyapatite, which is 8% [36]. This was due to the synthesis time which, when increased, favored the absorption of carbonate in the material, as well as the pH of the solution, since the solubility of CO_2 increases in more basic media [37].

The closest samples to the theoretical Ca/P ratio of 1.67 were HT11-6 h and MW9-1 min. However, only the HT11-12 h sample was above the Ca/P ratio of bone hydroxyapatite, which is between 1.5 and 1.85 [30,38].

Transmission electron microscopy

The TEM microstructures of the specimens selected by the two synthesis methods are shown in Fig. 4. For the

Table 2 – Results of crystal size calculation, carbonate percentage estimate and Ca/P ratio of hydroxyapatite samples.

Sample	Crystal size (nm)	% CO_3^{2-}	Ca/P
HT9-6 h	16.69	6.39	1.55
HT9-12 h	20.99	7.43	1.85
HT11-6 h	25.25	7.33	1.68
HT11-12 h	30.94	8.76	1.97
MW9-1 min	14.39	5.79	1.69
MW9-36 min	27.56	9.74	1.83
MW11-1 min	18.12	6.89	1.73
MW11-36 min	29.20	13.29	1.84

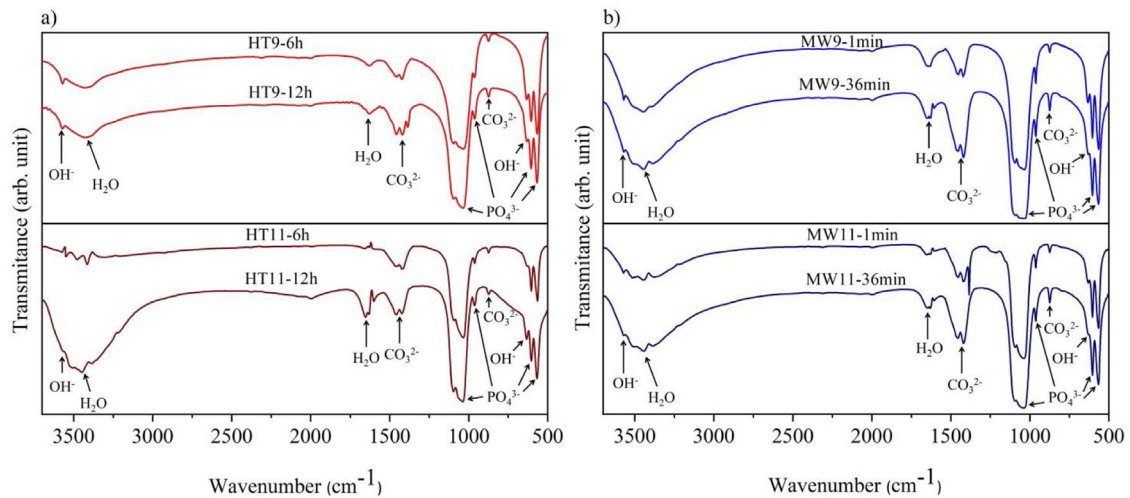


Fig. 3 – FTIR spectra of hydroxyapatite samples synthesized by (a) hydrothermal and (b) microwave irradiation.

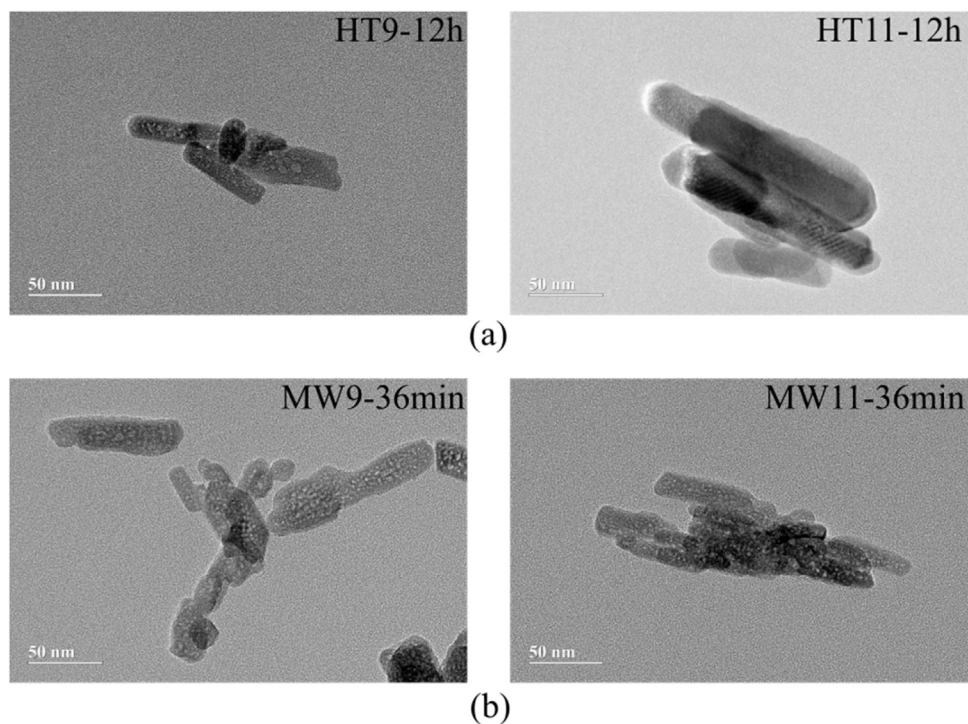


Fig. 4 – TEM micrographs of samples prepared by (a) HT and (b) MW.

hydrothermal method, it is possible to observe that well-defined nanorods were formed at both pHs. In the micrographs of the samples prepared by microwave irradiation there was also formation of nanorods, but much less defined and deformed.

The difference in the obtained morphologies by the two methods is related to the difference in the heating rate and synthesis time. This is due to in Hydrothermal synthesis the heating rate was slower and the synthesis time higher, which caused the hydroxyapatite particles to grow with more defined forms [39]. The Microwave Irradiation technique, because it has a faster heating rate, can cause rapid and

volumetric heating during material processing, accelerating particle nucleation that will be predominant to the growth rate, thus affecting its morphology [40,41].

The average particle size results were analyzed by TEM and are shown in the graph of Fig. 5. For Hydrothermal samples, an average particle size of 30 nm was obtained for the pH 9 and 50 nm synthesized sample for the sample at pH 11, corroborating with Guang et al. [34] and Bucur et al. [42]. In the samples prepared by Microwave irradiation at pH 9, the particles had an average size of 40 nm and at pH 11, 50 nm. Those results are similar to the one obtained by Kumar et al. [30] and Apalanga et al. [43].

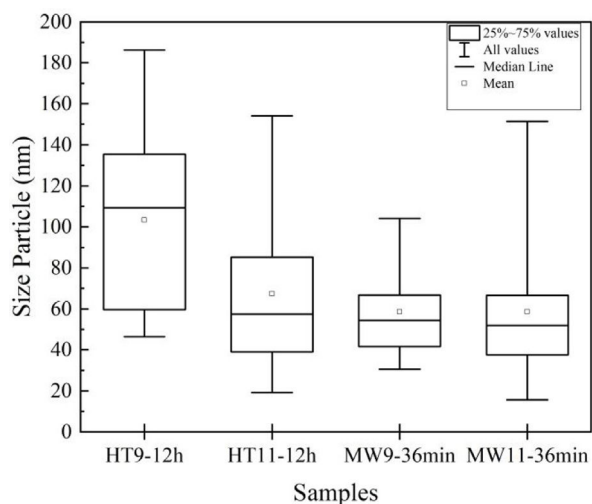


Fig. 5 – Particle size chart of HT9-12h, HT11-12h, MW9-3min and MW11-36min samples.

The nanorods morphology and a particle size between 20 and 80 nm of the synthesized material in this work have same characteristics of bone hydroxyapatite, which favors its application as a biomaterial in orthopedics implants.

Conclusion

Nanometric Hydroxyapatite powders were obtained using two synthesis methods: Hydrothermal and Microwave Irradiation from chicken eggshell residue as a biogenic source.

For both methods the pH and synthesis time parameters were varied in order to find possible differences between the obtained products. XRD analysis showed that all powders obtained were homogeneous, with only hydroxyapatite as the single phase.

FTIR results indicated the presence of hydroxyapatite common organic groups. The Ca/P ratio indicated that only the HT11-12h sample was above the stoichiometric ratio of bone hydroxyapatite.

TEM analysis revealed the formation of rod-like particles with particle sizes similar to bone mineral. The synthesized material at pH 9 presented better results in relation to the absorption of carbonates, which is the most recommended for the preparation of hydroxyapatite.

For the synthesis method, as the Hydrothermal generated more well-defined particles, and similar to bone hydroxyapatite, this can be considered the ideal method for hydroxyapatite synthesis route and further application as a bone graft biomaterial.

Acknowledgments

The authors thank the financial support of the Brazilian research financing institutions: CAPES, FAPEMA and the Federal Institute of Maranhão (IFMA). The Materials Analytical Center for XRD analysis and Chemistry Analytical Center for the FTIR analysis at Federal University Maranhão (UFMA). The

Analytical Physics Center from Federal University of Ceará (UFC) and the High-Resolution Microscopy Multi-User Laboratory at Federal University of Goiás.

REFERENCES

- [1] S.M. Zakaria, S.H.S. Zein, R. Othman, F. Yang, J.A. Jansen, Nanophase hydroxyapatite as a biomaterial in advanced hard tissue engineering: a review, *Tissue Eng. Part B-RE* 19 (2013) 431–441, <http://dx.doi.org/10.1089/ten.teb.2012.0624>.
- [2] J. Yazdani, E. Ahmadian, S. Sharifi, S. Shahi, S.M. Dizaj, A short view on nanohydroxyapatite as coating of dental implants, *Biomed. Pharmacother.* 105 (2018) 553–557, <http://dx.doi.org/10.1016/j.biopha.2018.06.013>.
- [3] J. He, K. Zhang, S. Wu, X. Cai, K. Chen, Y. Li, B. Sun, Y. Jia, F. Meng, Z. Jin, L. Kong, J. Liu, Performance of novel hydroxyapatite nanowires in treatment of fluoride contaminated water, *J. Hazard Mater.* 303 (2016) 119–130, <http://dx.doi.org/10.1016/j.jhazmat.2015.10.028>.
- [4] A. Fihri, C. Len, R.S. Varma, A. Solhy, Hydroxyapatite: a review of syntheses, structure and applications in heterogeneous catalysis, *Coordin. Chem. Ver.* 347 (2017) 48–76, <http://dx.doi.org/10.1016/j.ccr.2017.06.009>.
- [5] A.C. Ferro, M. Guedes, Mechanochemical synthesis of hydroxyapatite using cuttlefish bone and chicken eggshell as calcium precursors, *Mat. Sci. Eng. C* 97 (2019) 124–140, <http://dx.doi.org/10.1016/j.msec.2018.11.083>.
- [6] S. Pramanik, A.K. Agarwal, K.N. Rai, A. Garg, Development of high strength hydroxyapatite by solid-state-sintering process, *Ceram. Int.* 33 (2007) 419–426, <http://dx.doi.org/10.1016/j.ceramint.2005.10.025>.
- [7] S.K. Ghosh, S.K. Roy, B. Kundu, S. Datta, D. Basu, Synthesis of nano-sized hydroxyapatite powders through solution combustion route under different reaction conditions, *Mat. Sci. Eng. B* 176 (2011) 14–21, <http://dx.doi.org/10.1016/j.mseb.2010.08.006>.
- [8] J.S. Cho, Y.C. Kang, Nano-sized hydroxyapatite powders prepared by flame spray pyrolysis, *J. Alloys Comp.* 464 (2008) 282–287, <http://dx.doi.org/10.1016/j.jallcom.2007.09.092>.
- [9] Y. Qi, J. Shen, Q. Jiang, B. Jin, J. Chen, X. Zhang, The morphology control of hydroxyapatite microsphere at high pH values by hydrothermal method, *Adv. Powder Technol.* 26 (2015) 1041–1046. [doi:10.1016/j.apt.2015.04.008](https://doi.org/10.1016/j.apt.2015.04.008).
- [10] A. Yelten-Yilmaz, S. Yilmaz, Wet chemical precipitation synthesis of hydroxyapatite (HA) powders, *Ceram. Int.* 44 (2018) 9703–9710, <http://dx.doi.org/10.1016/j.ceramint.2018.02.201>.
- [11] S.K. Padmanabhan, A. Balakrishnan, M. Chu, Y.J. Lee, T.N. Kim, S. Cho, Sol-gel synthesis and characterization of hydroxyapatite nanorods, *Particuology* 7 (2009) 466–470, <http://dx.doi.org/10.1016/j.partic.2009.06.008>.
- [12] H. Zhou, J. Lee, Nanoscale hydroxyapatite particles for bone tissue engineering, *Acta Biomater.* 7 (2011) 2769–2781, <http://dx.doi.org/10.1016/j.actbio.2011.03.019>.
- [13] M. Sadat-Shojai, M.T. Khorasani, E. Dinpanah-Khoshdargi, A. Jamshidi, Synthesis methods for nanosized hydroxyapatite with diverse structures, *Acta Biomater.* 9 (2013) 7591–7621, <http://dx.doi.org/10.1016/j.actbio.2013.04.012>.
- [14] M.N. Hassan, M.M. Mahmoud, A.A. El-Fattah, S. Kandil, Microwave-assisted preparation of Nano-hydroxyapatite for bone substitutes, *Ceram. Int.* 42 (2016) 3725–3744, <http://dx.doi.org/10.1016/j.ceramint.2015.11.044>.
- [15] K. Salma-Ancane, L. Stipnicec, Z. Irbe, Effect of biogenic and synthetic starting materials on the structure of hydroxyapatite bioceramics, *Ceram. Int.* 42 (2016) 9504–9510, <http://dx.doi.org/10.1016/j.ceramint.2016.03.028>.

- [16] A.L. Adeogun, A.E. Ofudje, M.A. Idowu, S.O. Kareem, Facile development of nano size calcium hydroxyapatite based ceramic from eggshells: synthesis and characterization, *Waste Biomass Valori.* 9 (2018) 1469–1473, <http://dx.doi.org/10.1007/s12649-017-9891-3>.
- [17] D. Núñez, E. Elgueta, K. Varaprasad, P. Oyarzún, Hydroxyapatite nanocrystals synthesized from calcium rich bio-wastes, *Mater. Lett.* 230 (2018) 64–68, <http://dx.doi.org/10.1016/j.matlet.2018.07.077>.
- [18] H. Faridi, A. Arabhosseini, Application of eggshell wastes as valuable and utilizable products: a review, *Res. Agr. Eng.* 64 (2018) 104–114, <http://dx.doi.org/10.17221/6/2017-RAE>.
- [19] D.S.R. Krishna, A. Siddharthan, S.K. Seshadri, T.S.S. Kumar, A novel route for synthesis of nanocrystalline hydroxyapatite from eggshell waste, *J. Mater. Sci.-Mater. M* 18 (2007) 1735–1743, <http://dx.doi.org/10.1007/s10856-007-3069-7>.
- [20] J. Liu, X. Ye, H. Wang, M. Zhu, B. Wang, H. Yan, The influence of pH and temperature on the morphology of hydroxyapatite synthesized by hydrothermal method, *Ceram. Int.* 29 (2003) 629–633, [http://dx.doi.org/10.1016/S0272-8842\(02\)00210-9](http://dx.doi.org/10.1016/S0272-8842(02)00210-9).
- [21] Y.-Z. Wang, Y. Fu, Microwave-hydrothermal synthesis and characterization of hydroxyapatite nanocrystallites, *Mater. Lett.* 65 (2011) 3388–3390, <http://dx.doi.org/10.1016/j.matlet.2011.07.095>.
- [22] N. Méndez-Lozano, R. Velázquez-Castillo, E.M. Rivera-Muñoz, L. Bucio-Galindo, G. Mondragón-Galicia, A. Manzano-Ramírez, M.A. Ocampo, L.M. Apátiga-Castro, Crystal growth and structural analysis of hydroxyapatite nanofibers synthesized by the hydrothermal microwave-assisted method, *Ceram. Int.* 43 (2017) 451–457, <http://dx.doi.org/10.1016/j.ceramint.2016.09.179>.
- [23] N.K. Nga, N.T.T. Chau, P.H. Viet, Facile synthesis of hydroxyapatite nanoparticles mimicking biological apatite from eggshells for bone-tissue engineering, *Colloid Surf. B* 172 (2018) 769–778, <http://dx.doi.org/10.1016/j.colsurfb.2018.09.039>.
- [24] J.A. Rivera, G. Fetter, P. Bosch, Efecto del pH en la síntesis de hidroxiapatita en presencia de micro-ondas, *Rev. Matér.* 15 (2011) 506–515, <http://dx.doi.org/10.1590/S1517-70762010000400003>.
- [25] J.D.B. Featherstone, S. Pearson, R.Z. Legeros, An infrared method for quantification of carbonate in carbonated apatites, *Caries Res.* 18 (1984) 63–66, <http://dx.doi.org/10.1159/000260749>.
- [26] G.S. Kumar, A. Thamizhavel, E.K. Girija, Microwave conversion of eggshells into flower-like hydroxyapatite nanostructure for biomedical applications, *Mater. Lett.* 76 (2012) 198–200, <http://dx.doi.org/10.1016/j.matlet.2012.02.106>.
- [27] H. Yu, Y. Zhu, B.Q. Lu, Highly efficient and environmentally friendly microwave-assisted hydrothermal rapid synthesis of ultralong hydroxyapatite nanowires, *Ceram. Int.* 44 (2018) 12352–12356, <http://dx.doi.org/10.1016/j.ceramint.2018.04.022>.
- [28] J. Chen, Z. Wen, S. Zhong, Z. Wang, J. Wu, Q. Zhang, Synthesis of hydroxyapatite nanorods from abalone shells via hydrothermal solid-state conversion, *Mater. Des.* 87 (2015) 445–449, <http://dx.doi.org/10.1016/j.matdes.2015.08.056>.
- [29] S.J. Kalita, S. Verma, Nanocrystalline hydroxyapatite bioceramic using microwave radiation: synthesis and characterization, *Mater. Sci. Eng. C* 30 (2010) 295–303, <http://dx.doi.org/10.1016/j.msec.2009.11.007>.
- [30] G.S. Kumar, G. Karunakaran, E.K. Girija, E. Kolesnikov, N. Van Minh, M.V. Gorshenkov, D. Kuznetsov, Size and morphology-controlled synthesis of mesoporous hydroxyapatite nanocrystals by microwave-assisted hydrothermal method, *Ceram. Int.* 44 (2018) 11257–11264, <http://dx.doi.org/10.1016/j.ceramint.2018.03.170>.
- [31] B. Moreno-Perez, Z. Matamoros-Veloz, J.C. Rendon-Angeles, K. Yanagisawa, A. Onda, J.E. Perez-Terrazas, E.E. Mejia-Martinez, O.B. Diaz, M. Rodriguez-Reyes, Synthesis of silicon-substituted hydroxyapatite using hydrothermal process, *Bol. Soc. Esp. Ceram. Vidr.* 59 (2020) 50–64, <http://dx.doi.org/10.1016/j.bsecv.2019.07.001>.
- [32] W.H. Sutton, Microwave processing of ceramic materials, *Am. Ceram. Soc. Bull.* 68 (1989) 376–386, <http://dx.doi.org/10.1017/S0883769400038495>.
- [33] M.F. Alif, W. Aprillia, S. Arief, A hydrothermal synthesis of natural hydroxyapatite obtained from *Corbicula moltkiana* freshwater clams shell biowaste, *Mater. Lett.* 230 (2018) 40–43, <http://dx.doi.org/10.1016/j.matlet.2018.07.034>.
- [34] S. Guang, F. Ke, Y. Shen, Controlled preparation and formation mechanism of hydroxyapatite nanoparticles under different hydrothermal conditions, *J. Mater. Sci. Technol.* 31 (2015) 852–856, <http://dx.doi.org/10.1016/j.jmst.2014.12.013>.
- [35] A. Paz, D. Guadarrama, M. López, J.E. González, N. Brizuela, J. Aragón, A comparative study of hydroxyapatite nanoparticles synthesized by different routes, *Quim. Nova* 35 (2012) 1724–1727, <http://dx.doi.org/10.1590/S0100-40422012000900004>.
- [36] S. Markovic, L. Veselinovic, M.J. Lukic, L. Karanovic, I. Bracko, N. Ignjatovic, D. Uskokovic, Synthetical bone-like and biological hydroxyapatites: a comparative study of crystal structure and morphology, *Biomed. Mater.* 6 (2011) 1–14, <http://dx.doi.org/10.1088/1748-6041/6/4/045005>.
- [37] J.D. Hem, Significance of properties and constituents reported in water analysis, in: J.D. Hem (Ed.), *Study and Interpretation of the Chemical Characteristics of Natural Water*, U.S. Geological Survey, USA, 1985, pp. 106–162.
- [38] S.-C. Wu, H.-K. Tsou, H.-C. Hsu, S.-K. Hsu, S.-P. Liou, W.-F. Ho, A hydrothermal synthesis of eggshell and fruit waste extract to produce nanosized hydroxyapatite, *Ceram. Int.* 39 (2013) 8183–8188, <http://dx.doi.org/10.1016/j.ceramint.2013.03.094>.
- [39] R. Zhu, R. Yu, J. Yao, D. Wang, J. Ke, Morphology control of hydroxyapatite through hydrothermal process, *J. Alloys Comp.* 457 (2008) 555–559, <http://dx.doi.org/10.1016/j.jallcom.2007.03.081>.
- [40] S.H. Jung, T. Jin, Y.K. Hwang, J.-S. Chang, Microwave effect in the fast synthesis of microporous materials: which stage between nucleation and crystal growth is accelerated by microwave irradiation? *Chem. Eur. J.* 13 (2007) 4410–4417, [doi:10.1002/chem.200700098](http://dx.doi.org/10.1002/chem.200700098).
- [41] I. Bilecka, M. Niederberger, Microwave chemistry for inorganic nanomaterials synthesis, *Nanoscale* 2 (2010) 1358–1374, <http://dx.doi.org/10.1039/b9nr7k0037>.
- [42] A.I. Bucur, R.A. Bucur, Z. Szabadai, C. Mosoarca, P.A. Linul, Influence of small concentration addition of tartaric acid on the 220 °C hydrothermal synthesis of hydroxyapatite, *Mater. Charact.* 132 (2017) 76–82, <http://dx.doi.org/10.1016/j.matchar.07.047>.
- [43] V. Apalangya, V. Rangari, S. Jeelani, E. Dankyi, A. Yaya, S. Darko, Rapid microwave synthesis of needle-like hydroxyapatite nanoparticles via template directing ball-milled spindle-shaped eggshell particles, *Ceram. Int.* 44 (2018) 7165–7171, <http://dx.doi.org/10.1016/j.ceramint.01.161>.